Proceedings of the ASME 2017 36th International Conference on Ocean, Offshore and Arctic Engineering
OMAE2017
June 25-30, 2017, Trondheim, Norway

OMAE2017-61768

VIV RESPONSES OF RISER WITH BUOYANCY ELEMENTS: FORCED MOTION TEST AND NUMERICAL PREDICTION

Jie Wu
SINTEF Ocean[1)]
Trondheim, Norway

Halvor Lie
SINTEF Ocean
Trondheim, Norway

ShiXiao Fu
SINTEF Ocean
Trondheim, Norway

Rolf Baarholm
Statoil
Trondheim, Norway

Yiannis Constantinides
Chevron
Houston, USA

1) Formerly MARINTEK. SINTEF Ocean from January 1st 2017 through an internal merger in the SINTEF Group

ABSTRACT

Steel Lazy Wave Riser (SLWR) is an attractive deep water riser concept. When subjected to vortex induced vibrations (VIV), the vortex shedding process of the buoyancy element and the bare riser section will be different due to the difference in diameter. VIV responses can be strongly influenced by the dimension of the buoyancy element and its arrangement.

Empirical VIV prediction programs, such as VIVANA, SHEAR7 and VIVA, are widely used by the industry for design against VIV loads. However, there is lack of hydrodynamic data to be used in these programs when buoyancy elements are present.

Experiment to obtain hydrodynamic data for riser with staggered buoyancy elements was carried out in the towing tank in SINTEF Ocean. A rigid cylinder section with three staggered buoyancy elements was subjected to harmonic forced cross-flow (CF) motions. Hydrodynamic forces on one of the buoyancy elements were directly measured in addition to the measured forces at both ends of the test section. Two buoyancy element configurations were tested and the corresponding hydrodynamic data are compared with that of a bare cylinder. The obtained hydrodynamic data was also used in VIV prediction software and good prediction against existing flexible cylinder staggered buoyancy element VIV test data was achieved. A roadmap to achieve an optimal SLWR design by combining different experimental and numerical methods is suggested.

NOMENCLATURE

VIV	Vortex induced vibration
CF	Cross-flow
IL	In-line
Re	Reynolds number
F_d	Drag force
C_d	Drag coefficient
C_e	Excitation (lift) coefficient
C_a	Added mass coefficient
A	Displacement amplitude (m)
L_r, L_b	Length of the bare riser, buoyancy element (m)
L_c	Spacing between two buoyancy elements (m)
D_r, D_b	Diameter of the bare riser, buoyancy element (m)
U	Towing speed (m/s)
f_{osc}	Oscillation frequency of the test cylinder (Hz)
$\bar{f}$	Non-dimensional (normalized) frequency, $\bar{f} = \frac{f_{osc}D}{U}$
U_r	Reduced velocity, $U_r = \frac{U}{f_{osc}D}$
k	Roughness of the surface (m)

INTRODUCTION

When a SLWR is subjected to current, both the buoyancy elements and the riser may experience VIV. The vortex shedding process from the riser and the buoyancy element will also interact.

Several model tests were carried out to study the interaction of bare pipe section and buoyancy elements and its effect on VIV, Lie, et al, 1998, Li, et al, 2011, Jhingran, et al, 2012, Rao, et al 2015. The Norwegian Deepwater Program (NDP) recently performed scaled model tests with 38 m riser model with staggered buoyancy elements in SINTEF Ocean's Ocean Basin in 2014 (Wu, et al 2016a). In these tests, the acceleration and bending strains are normally measured. The study of the test data shows that the interaction can be influenced by many parameters, such as the arrangement of the buoyancy element, aspect ratio of the buoyancy element, etc. There is a competition between the vortex induced forces acting on the buoyancy element and the riser segment. By proper design, the total VIV response can be reduced by tuning this competition. There is a challenge to achieve an optimal design and arrangement for staggered buoyancy elements with minimum VIV responses.

Computational Fluid Dyanmics (CFD) has been used to evaluate the VIV responses of SLWR by Constantinides, et al (2014, 2016) and compared with existing model tests.

Empirical VIV prediction programs, such as VIVANA (Passano, et al 2014), Shear7 (Vandiver & Li, 2007) and VIVA (Triantafyllou, et al 1999), still lack of hydrodynamic data to predict VIV responses for riser with staggered buoyancy elements.

Inverse analysis is an effective method to extract hydrodynamic force coefficient from experiment with flexible cylinders using measured responses, (Wu, 2011, Wu, et al 2016c, Song, et al 2016). Significant improvement in VIV prediction with the obtained hydrodynamic data has been achieved (Wu, 2011). It has also been applied to analyze VIV data from the testing of flexible cylinder with staggered buoyancy elements (Fu, et al 2017).

In present study, rigid cylinder forced motion experiment to obtain hydrodynamic data for riser with staggered buoyancy elements were presented. The obtained hydrodynamic data was used in VIVANA and the prediction results were compared with NDP 38m pipe tests with staggered buoyancy elements (Wu, et al, 2016a, Voie, et al 2017).

MODEL TEST

Model tests with rigid cylinder were performed, which consists of stationary and forced motion tests. The test cylinder was towed in still water in the stationary test. While, the cylinder was forced to oscillate in CF direction during the forced motion test. Hydrodynamic forces for buoyancy element and bare riser are measured. Hydrodynamic force coefficients, e.g. drag, excitation and added mass coefficients, were estimated.

Test Setup

The test rig was connected to the Hexapod, which was used to provided desired motions (see Figure 1). A test rig was fixed below the Hexapod. The test cylinder can be seen between two end plates in the figure. The length of the test section is 1.05 m; however, the test rig is adjustable to accommodate a longer test section.

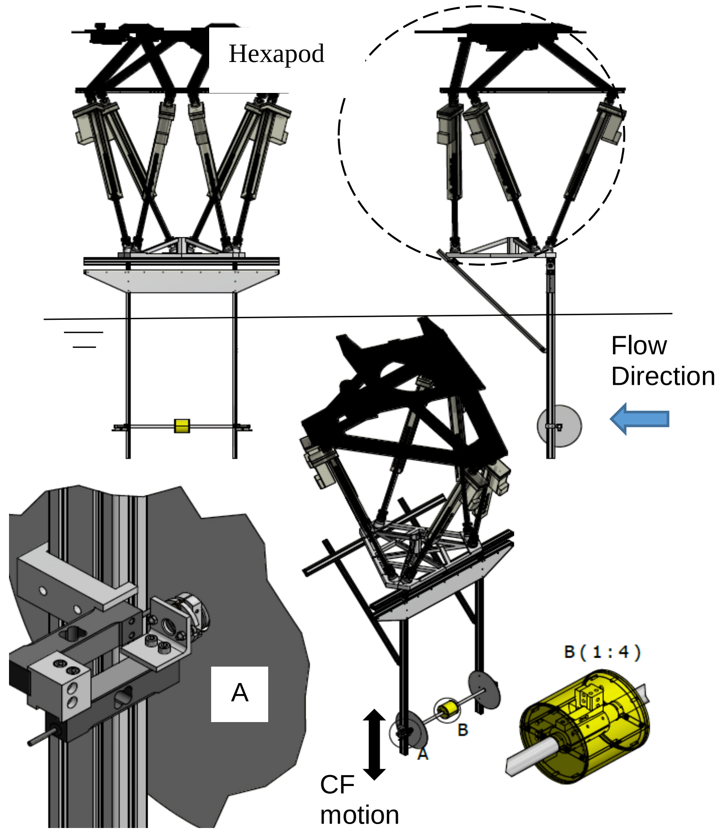

Figure 1 Test setup

Riser Models

The bare riser is made of steel. The outer diameter is 0.03 m and the length is 1.05 m. The length over diameter ratio (L_r/D_r) is 35.

The buoyancy element is made of ABS material. The length of each element is 0.15 m and the diameter is 0.15 m. The aspect ratio (L_b/D_b) of one element is 1.0. The diameter ratio between the buoyancy element and the riser diameter (D_b/D_r), is 5.

Test Configurations

Four configurations are tested, as shown in Figure 2. The bare cylinder and full buoyancy configurations were used to validate the test setup by comparing the results with the existing literature. Two staggered buoyancy element configurations were tested. Due to the large difference in diameter between the buoyancy element and the bare riser $(D_b/D_r = 5/1)$, the vortex shedding frequencies will be significantly different. It means that when the buoyancy element is excited, the bare riser section will be in the damping region, and vice visa. Therefore, two set of tests were carried out for configurations with staggered buoyancy elements so that the bare riser section and buoyancy element can be excited individually.

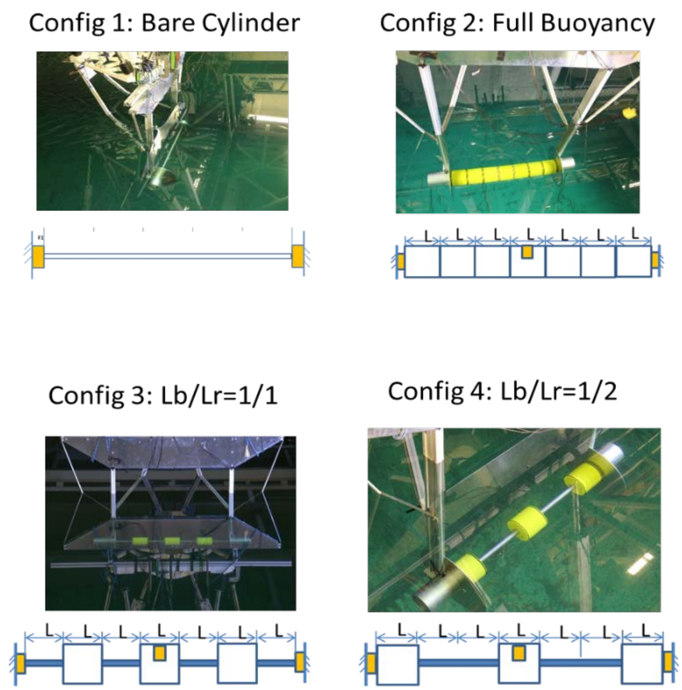

Figure 2 Test configurations

Instrumentations

Two 2-component force transducers are installed at the end of the test pipe (see also in view A in Figure 1). For tests with buoyancy elements, an additional 2-component force transducer is installed connecting the buoyancy element and the bare riser section, as shown in view B in Figure 1. A 3-component accelerometer was positioned close to the end plate to monitor the vibrations of the test rig. An optical tracking system (OQUS) was used to measure the movement of the test rig, in addition to the direct output data from Hexapod. The sampling frequency of the force transducer and the accelerometer is 200 Hz. The sampling frequency of the Hexapod and the OQUS system is 100 Hz and 50 Hz, respectively.

Hydrodynamic Data from Model Test

The hydrodynamic forces are derived from measured forces and the inertial loads are subtracted. The excitation, added mass and drag coefficients for the bare riser and the buoyancy elements are calculated individually, refer to Table 1. Some of the results are selected to be presented in this section.

Table 1 Summary of hydrodynamic data from model tests

Configuration	Stationary Test	Forced Motion Test	
		Riser frequency excitation	Buoyancy frequency excitation
Config. 1 (bare)	Cd	Cd, Ce, Ca	Cd, Ce, Ca
Config. 2* (full buoyancy)	Cd	N/A	N/A
Config. 3 (Lb/Lr=1/1)	Cd (buoyancy) Cd (total)	Cd, Ce, Ca (riser) Cd, Ce, Ca (buoyancy)	Cd, Ce, Ca (riser) Cd, Ce, Ca (buoyancy)
Config. 4 (Lb/Lr=1/2)	Cd (buoyancy) Cd (total)	Cd, Ce, Ca (riser) Cd, Ce, Ca (buoyancy)	Cd, Ce, Ca (riser) Cd, Ce, Ca (buoyancy)

Drag Coefficient

1) Drag Coefficient from Stationary Test

The drag coefficient of a fixed rigid cylinder can be found in (DNV, 2010), shown in Figure 3.

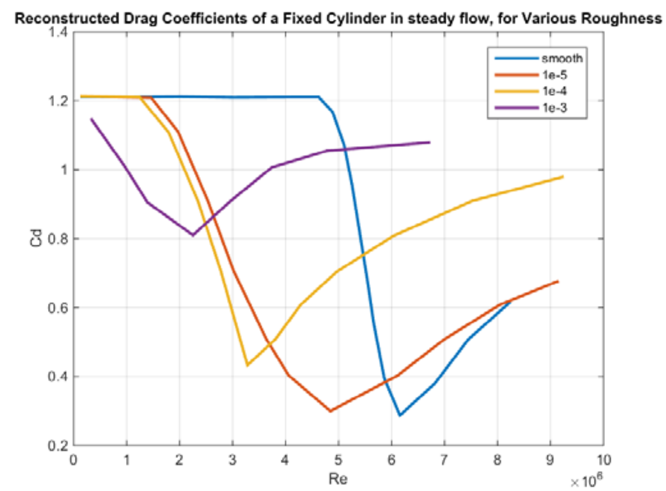

Figure 3 Reconstructed drag coefficients from stationary test for cylinder with various roughness (DNV, 2010)

The reduction factor for drag force of a circular cylinder (L/D=2) in subcritical flow is 0.58 compared to that of an infinitely long cylinder (DNV, 2010).

The test section was fixed and towed in still water. The drag coefficients vs. Reynolds number are presented in Figure 4. The bare riser is made of steel (uncoated) and its roughness is about $k/D = 5 \times 10^{-5}$ (DNV, 2010). The highest towing speed for the bare cylinder configuration is 1.5 m/s without interfering with the natural frequency of the rig. The measured drag coefficients (green circles) falls between the data corresponding to a smooth cylinder and a cylinder with roughness ratio ($k/D = 1 \times 10^{-5}$) in Figure 3 in the Reynolds number range $Re \approx 8 \times 10^3 - 4 \times 10^4$. The drag coefficients of full buoyancy configuration (Config.2) are represented by the purple diamonds in the figure.

Seven buoyancy elements are placed together in this configuration. It is noted that the surface of the buoyancy element is made of ABS material and the alignment between two neighboring buoyancy elements is not perfect. The influence on the drag coefficient is difficult to evaluate. It is therefore not further commented. No forced motion test was carried out for full buoyancy configuration.

The hydrodynamic forces on the middle buoyancy element F_b were directly measured. The corresponding drag coefficient for this buoyancy element is calculated $C_{db} = \frac{F_b}{\frac{1}{2}\rho {D_b}^2 U^2}$. C_{db} is about 0.7 for the last two configurations (blue and yellow data points). There is no data in literature for direct comparison. If the reduction factor 0.58 is used, the theoretical drag coefficient of the buoyancy element is about 0.66 at $Re \approx 4 \times 10^4$. The actual buoyancy element in present test has a shorter aspect ratio $\frac{L_b}{D_b} =$ 1.0.

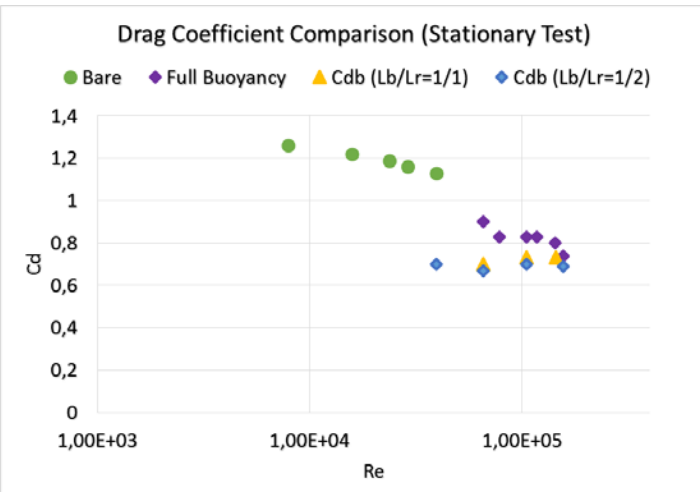

Figure 4 Drag coefficients from stationary test

2) Drag Coefficient from Forced Motion Test

The drag coefficients obtained from the bare riser configuration are presented in Figure 5. These values compare well with the data in literature (Gopalkrishnan, 1992).

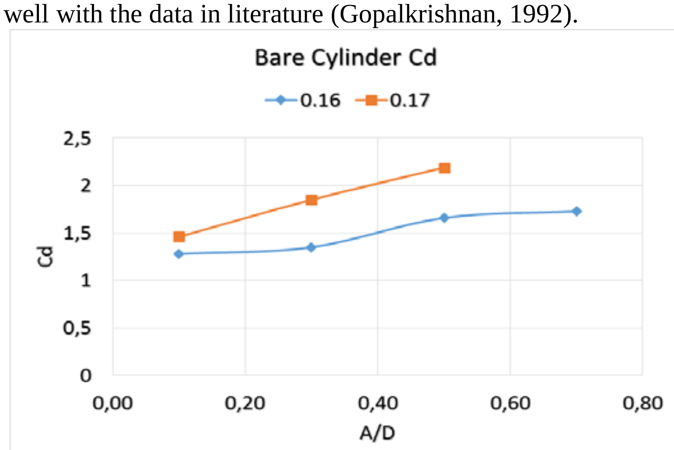

Figure 5 Drag coefficients of bare riser from forced motion test. Different colours represent different $\bar{f}$.

The drag coefficients for config. 3 subjected to buoyancy frequency excitation are presented in Figure 6. The averaged drag coefficient is about 0.7 at smallest amplitude, which is similar to the drag coefficient when it is stationary, see also Figure 4. The values increase with motion amplitude, as expected. The drag coefficient subjected riser frequency excitation is shown in Figure 7. The averaged C_d value is about 0.7 and the variation is small due to small displacements.

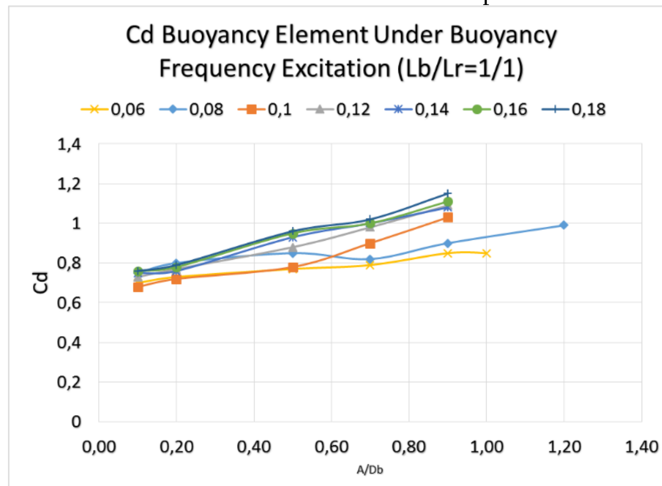

Figure 6 Drag coefficients of the buoyancy element: Lb/Lr=1/1, under buoyancy frequency excitation. Different colours represent different $\bar{f}$.

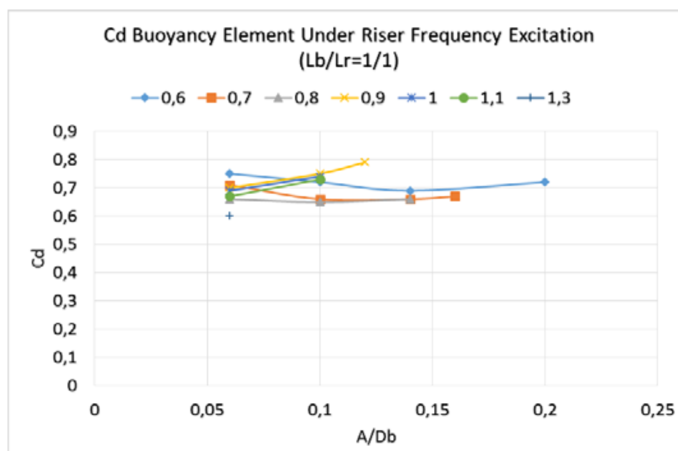

Figure 7 Drag coefficients of the buoyancy element: Lb/Lr=1/1, under riser frequency excitation. Different colours represent different $\bar{f}$.

Excitation Coefficient

The excitation (lift) coefficient corresponds to the hydrodynamic force, which is in-phase with velocity. Diameter of the buoyancy element and bare riser section are used in the calculation of excitation coefficients for the buoyancy element and bare riser section respectively.

1) Excitation Coefficient of a Bare riser (Config.1)

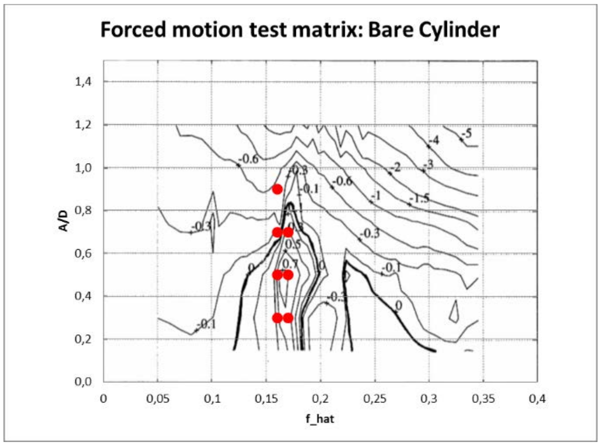

Figure 8 Test matrix for bare cylinder forced motion test. Red dots represent test cases.

The estimated excitation coefficients C_e (orange and blue data points) for the bare riser at two $\bar{f} = \frac{f_{osc}D}{U}$ with different displacement amplitudes are presented in Figure 9. These data are compared with interpolated values from literature (Gopalkrishnan, 1992) in the same figure. The discrepancy may be partially due to the uncertainty in the interpolation in the excitation region of $\bar{f} \approx 0.16 - 0.17$. The highest C_e value is about 0.82 at $\bar{f} \approx 0.165$. This is close to $C_e = 0.89$ taken at $\bar{f} \approx 0.17$ from present test. This comparison shows that the test rig and the measurement is reliable.

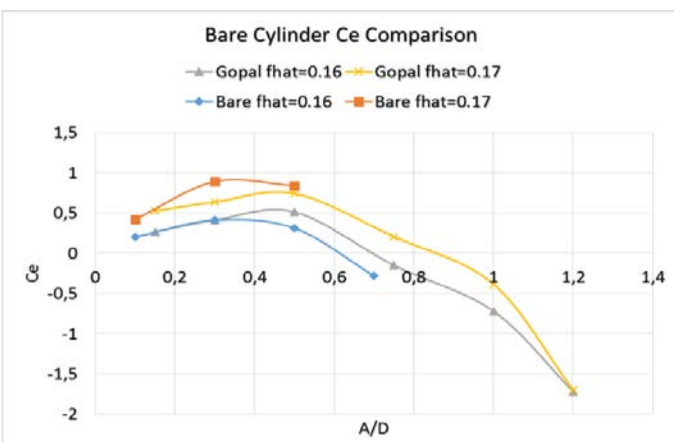

Figure 9 Excitation coefficients for a bare riser (Config. 1)

2) Excitation Coefficient of Staggered Buoyancy Configuration, Lb/Lr=1/1 (Config.3)

The design of the test matrix is based on the results of the flexible cylinder model tests with staggered buoyancy elements (Wu, et al, 2016). It shows that the buoyancy element has a significantly lower shedding frequency due to its short aspect ratio. This means that the corresponding non-dimensional frequency of the buoyancy element is lower. The test matrix is presented in Figure 10.

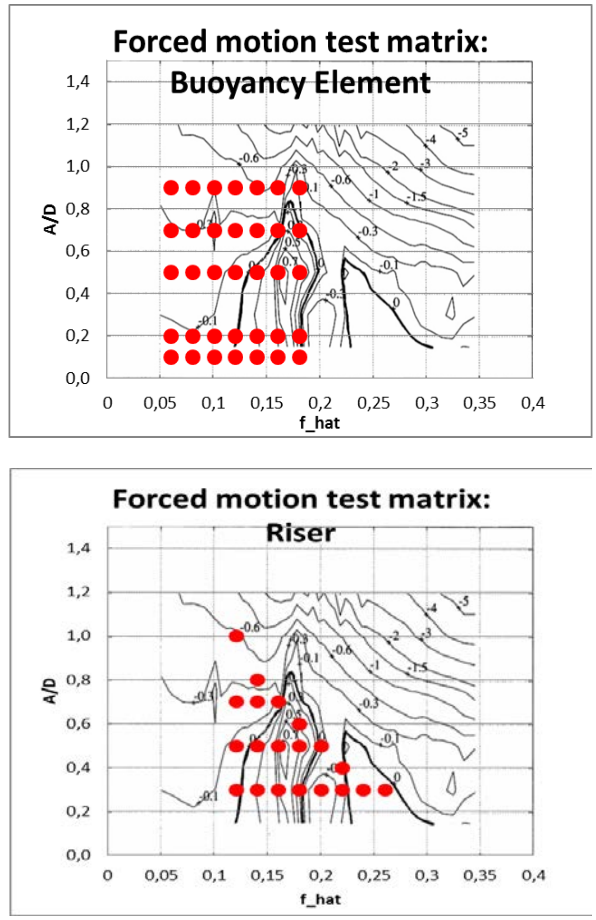

Figure 10 Test matrix for forced motion test of config. 3 (Lb/Lr=1/1)

The excitation coefficients are presented in Figure 11 to Figure 14. Several observations could be made based on these results:

- Excitation region for buoyancy element is observed for $\bar{f} \approx 0.06 - 0.12$. The maximum A/D corresponding to zero excitation coefficient can reach 1.2 D_b or 6.0 D_r. The maximum C_e for the buoyancy element is about 0.2 at $\bar{f} = 0.08$.
- When buoyancy element is excited, bare riser section will provide damping force and vice versa.
- The aspect ratio of the bare riser section (L_r/D_r) between two buoyancy elements is 5. The buoyancy elements act as end plates. The excitation coefficient of bare riser section is close to a rigid cylinder with end plates. The maximum C_e for the riser section is about 0.5 at $\bar{f} = 0.18$.

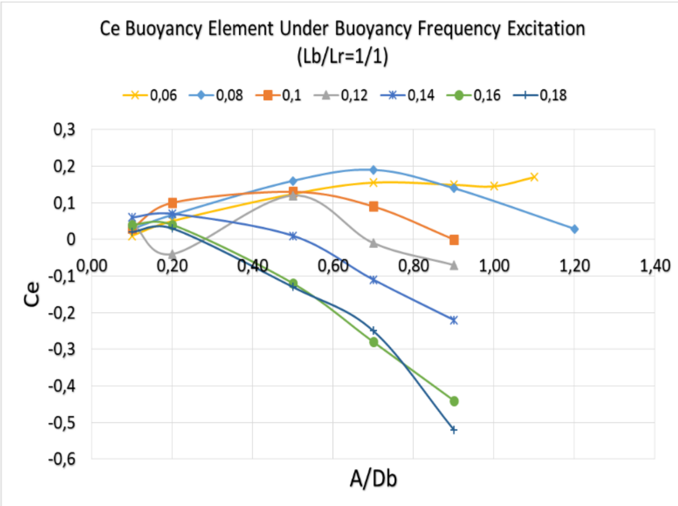

Figure 11 Excitation coefficients for buoyancy element: Config. 3, Lb/Lr=1/1, under buoyancy frequency excitation

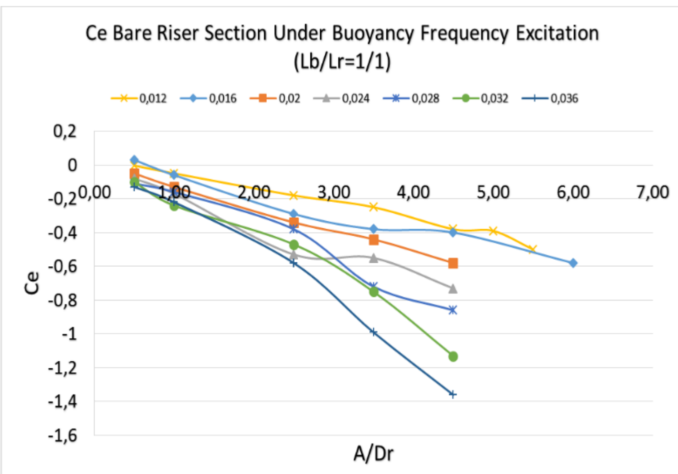

Figure 12 Excitation coefficients for bare riser section: Config. 3, Lb/Lr=1/1, under buoyancy frequency excitation

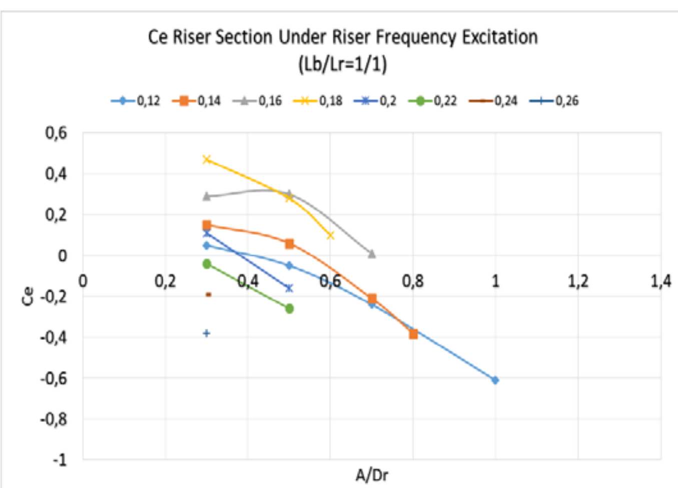

Figure 13 Excitation coefficients for bare riser section: Config. 3, Lb/Lr=1/1, under riser frequency excitation

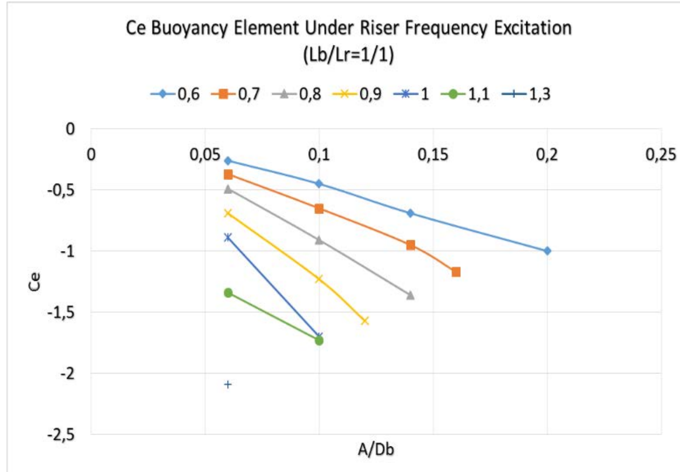

Figure 14 Excitation coefficients for buoyancy element: Config. 3, Lb/Lr=1/1, under riser frequency excitation

3) Damping Coefficient of Staggered Buoyancy Configuration, Lb/Lr=1/1 (Config.3)

(Venugopal, 1996) predicts the damping force for a rigid cylinder oscillating in still water, at velocities lower than the excitation velocity range, and at higher. This model was based on published empirical damping data from sub-critical flow experiments. This model is applied for CF and IL response calculations when the cross-section is in outside of the excitation range. (Vikestad, Larsen, & Vandiver, 2000) has shown the damping force from Venugopal's model can be expressed by the equivalent excitation coefficients, assuming zero flow speed.

The damping can be expressed using excitation (lift) coefficients. The converted low/high velocity damping coefficient based on the oscillation frequency/amplitude of the test is presented in Figure 15 and Figure 16, respectively. Venugopal's low velocity damping model is a function of both motion amplitude and frequency. By comparing Figure 14 and Figure 15, it can be seen that buoyancy element provides more damping than what is estimated based on Venugopal's model. The comparison between Figure 12 and Figure 16 shows that the bare riser section provides less damping than the damping model's estimation. Venugopal's (1996) damping model can be used with correction factors based on experiment data.

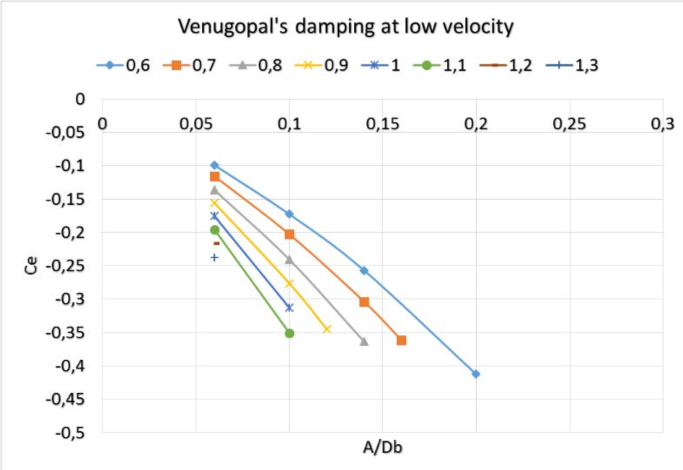

Figure 15 Converted negative excitation coefficients at low velocity

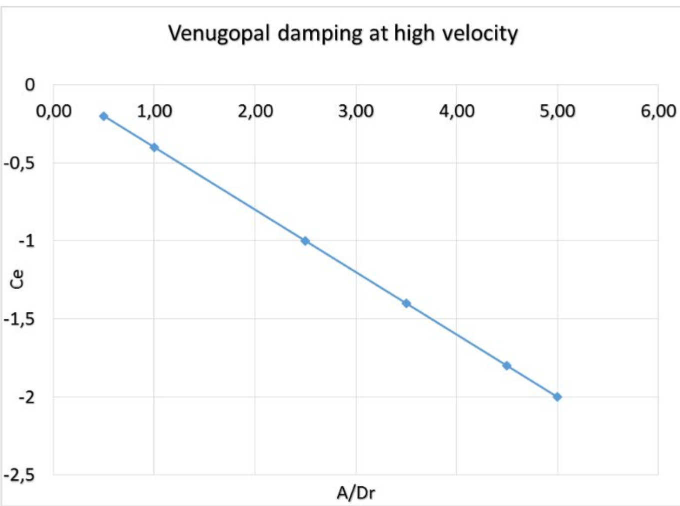

Figure 16 Converted negative excitation coefficients at high velocity

4) Added mass Coefficient of Staggered Buoyancy Configuration, Lb/Lr=1/1 (Config.3)

The added mass coefficients were presented against displacement amplitude ratio in Figure 17. It can be seen that the added mass of the bare riser section has an averaged value around 10, which is significantly different that that from bare cylinder tests (Gopalkrishnan, 1992).

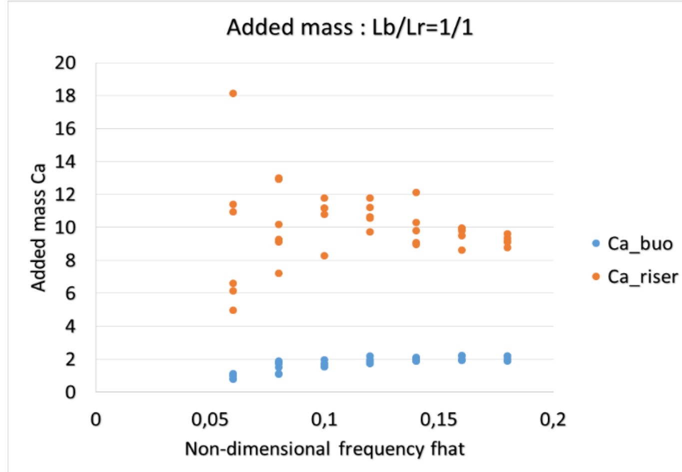

Figure 17 Added mass coefficients: Config. 3, Lb/Lr=1/1, under riser frequency excitation

5) Hydrodynamic Force Coefficient of Staggered Buoyancy Configuration, Lb/Lr=1/2 (Config.4)

The major difference in the force coefficients when the spacing between two buoyancy elements increase to Lb/Lr=1/2 is that there is no positive excitation for the buoyancy element. This seems to explain the observation from the flexible cylinder tests, where there is no VIV responses at buoyancy frequency when the spacing is increased (Wu, et al 2016a). The detailed results for this configuration could be found in (Wu, et al 2016b).

NUMERICAL ANALYSIS

The hydrodynamic data generalized from the rigid cylinder forced motion test are now used in numerical prediction of a flexible pipe with staggered buoyancy elements and compared with existing flexible pipe model test data.

Semi-empirical VIV Prediction Program VIVANA

VIVANA is a semi-empirical coefficient based program for estimation of VIV of slender marine structures developed by SINTEF Ocean and NTNU. The structure is modeled using finite elements and the response found in the frequency domain. A more detailed description of VIVANA can be found in Passano, et al (2014).

The response calculations are carried out at discrete response frequencies. The main VIV coefficients are the CF and IL excitation, added mass and damping coefficients.

Construction of Hydrodynamic Force Database

Based on the model test results in previous section, the excitation, added mass and damping model are defined as input for the prediction program VIVANA. These parameters are used to predict the VIV response of a flexible cylinder with staggered buoyancy element and compared with experimental data.

Table 2 Summary of the input parameters

Config.	Excitation coefficient		Excitation zone $\bar{f}$		Added mass	
	Riser	Buo.	Riser	Buo.	Riser	Buo.
Lb/Lr=1/1	Ce curve 1	Ce curve 2	0.16-0.22	0.06-0.12	10.0	2.0
Lb/Lr=1/2	Ce curve 1	N/A	0.16-0.22	N/A	10.0	2.0

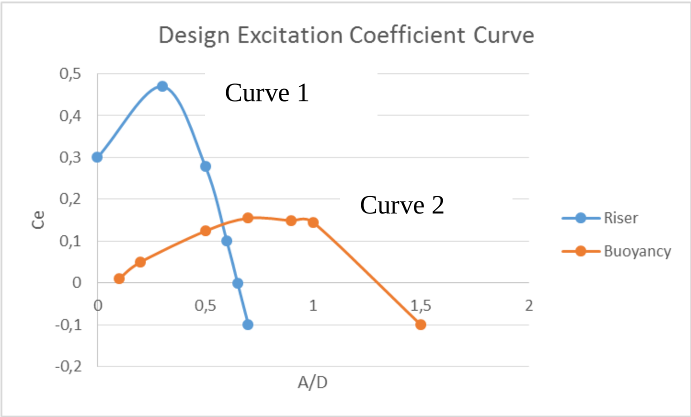

Figure 18 Design curves of the excitation coefficient

VIVANA Prediction

Riser with staggered buoyancy elements are explicitly modelled in VIVANA. The predicted responses (frequency, fatigue damage) are compared with NDP 38m flexible cylinder with staggered buoyancy element test data (Wu, et al, 2016a). The hydrodynamic data can also be used by other VIV prediction programs as well.

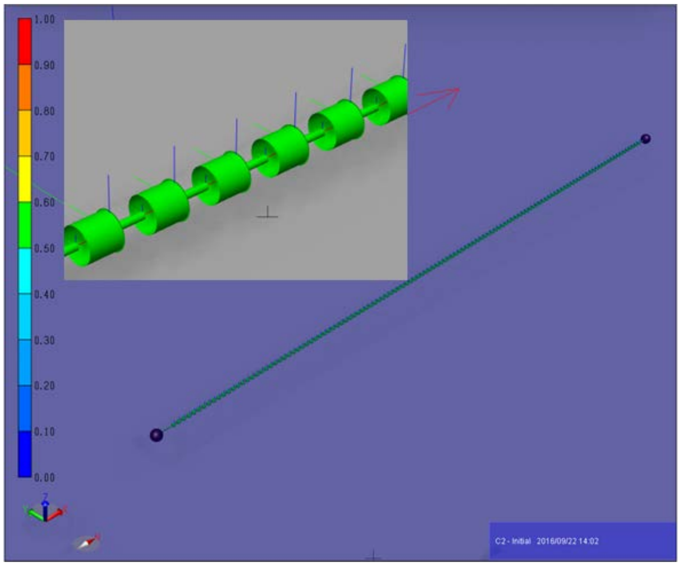

Figure 19 VIVANA/SIMA model of the riser with staggered buoyancy elements

The tested flexible cylinder configurations are shown in Figure 20. Two test configurations (C1 and C2) are selected to be evaluated.

Configuration	3	6	1	5	2	4
Spacing Ratio (Lc/Lb)	3/1	2/1	2/1	1/1	1/1	2/1
Aspect Ratio (Lb/Db)	1/1	1/1	1/1	2/1	1/1	1/1
Diameter Ratio (Db/Dr)	5/1	5/1	5/1	5/1	5/1	5/1
Coverage (%)	25	17 (half bare)	33	50	50	17 (half strake)
Schematic drawing						

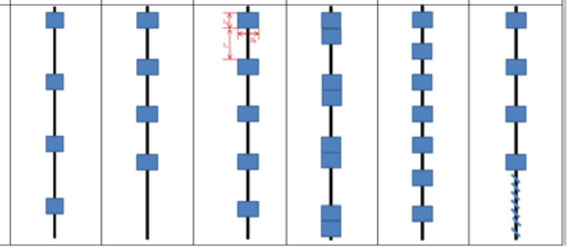

Figure 20 Schematic drawing of test configurations (Wu, et al, 2016)

The comparison of the dominating frequency and maximum fatigue damage of configuration C2 are presented in Figure 21 and Figure 22. Both indicate that the design parameters can give good predictions compared to the model test results. The displacement comparison is presented in Figure 23. It can be seen that the displacement is under-predicted. However, the under-prediction at buoyancy element frequency does not influence the total fatigue damage, due to its low mode response. The discrepancy in fatigue damage prediction is within a factor of 2.0 for most of the cases.

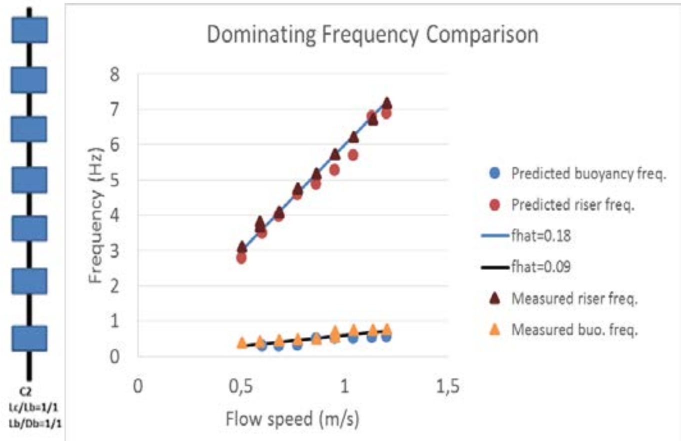

Figure 21 Dominating frequency prediction for NDP 38m staggered buoyancy test C2. Lb/Lr=1/1

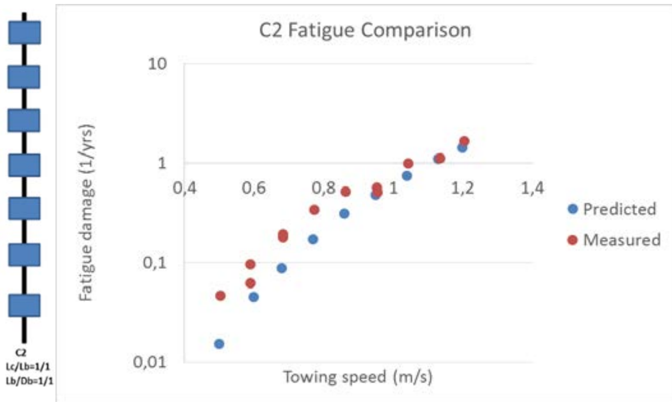

Figure 22 Maximum fatigue damage prediction for NDP 38m staggered buoyancy test C2. Lb/Lr =1/1

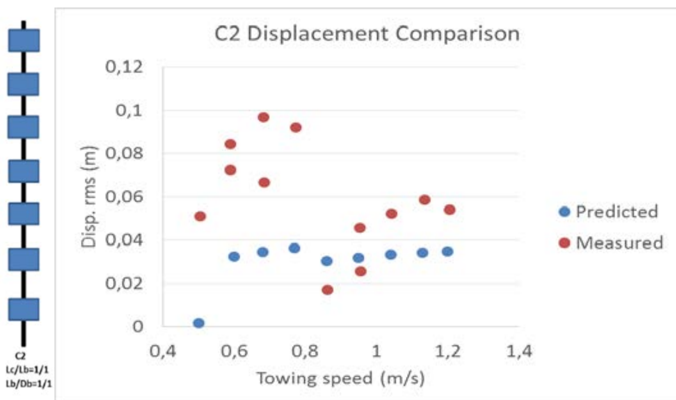

Figure 23 Maximum displacement amplitude prediction for NDP 38m staggered buoyancy test C2. Lb/Lr =1/1

The comparison of maximum fatigue damage prediction for configuration C1 is shown in Figure 24. The discrepancy is within a factor of 2.5 for most of the cases. It can be seen that the fatigue damage for C1 configuration is slightly higher that of C2 at higher towing speed. Such analysis helps to select the optimal buoyancy element design.

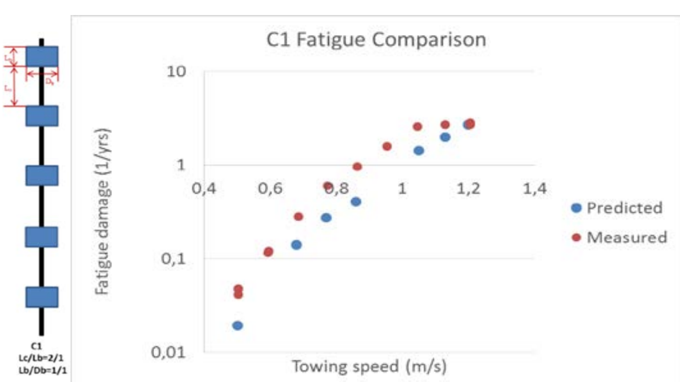

Figure 24 Maximum displacement amplitude prediction for NDP 38m staggered buoyancy test C1. Lb/Lr =1/2

CONCLUSIONS

Experiment and numerical study have been performed to obtain hydrodynamic data for riser with staggered buoyancy elements. Some of the major findings are summarized below.

Rigid cylinder forced motion tests with staggered buoyancy elements are shown to be a cost effective method to investigate the interaction between buoyancy elements and bare riser section compared to a more complicated flexible cylinder test. Such interaction are shown to have significant influences on the VIV responses and force coefficients, depending on the dimension of the buoyancy element and its arrangement. The new feature of such test is that an additional force transducer is placed inside the buoyancy element to measure the hydrodynamic force on the buoyancy element directly. The obtained hydrodynamic force coefficient data has been used in VIV prediction programs and predicted fatigue damage compare well with existing flexible cylinder VIV tests with staggered buoyancy elements.

It seems to be fruitful to combine different experimental and numerical method to achieve an optimal SLWR design.

1) Systematic screening of potential staggered buoyancy element configurations with forced motion tests.
2) Construct hydrodynamic database based on forced motion test data.
3) Numerical evaluation of SLWR design concepts with constructed database and select optimal designs.
4) Validation of design with flexible cylinder model tests.
5) Analysis of flexible cylinder model tests with inverse analysis and improve numerical predictions.

ACKNOWLEDGMENTS

The authors are grateful to the financial support of the Norwegian Deepwater Program (NDP) and its permission to publish this study.

REFERENCES

[1] Constantinides, Y. and Zhang, M., VIV assessment of deepwater lazy-wave risers. OMAE2014-24522.

[2] Constantinides, Y., Stover, M., Steele, A. and Santala, M., CFD Modeling and Validation of Steel Lazy-Wave Riser VIV. 35th International Conference on Ocean, Offshore and Arctic Engineering, OMAE2016-54945.

[3] DNV. (2010). RP-C205: Environmental conditions and environmental loads.

[4] Fu, S., Lie, H., Wu, J., Baarholm, R., Zhang, M., Hydrodynamic Coefficients in Cross Flow Direction of a Flexible Pipe with Staggered Buoyancy Modules under VIV Conditions by Inverse Analysis. OMAE2017.

[5] Gopalkrishnan, R. (1992). Vortex-Induced Forces on Oscillating Bluff Cylinders. Cambridge, MA, USA: Massachusetts Institute of Technology.

[6] Gouda, B.H.L., "Some Measurements of the Phenomena Vortex-Shedding and Induced Vibrations of Circular Cylinders", Technische Universitat Berlin, Report DLR-FB 75-01, 1975

[7] Voie, P., Wu, J., Larsen, C.M., Resvanis,T., Vandiver, K., and Triantafyllou, M., Consolidated guideline on analysis of vortex-induced vibrations in risers and umbilicals, Trondheim, 36th International Conference on Ocean, Offshore and Arctic Engineering, OMAE2017-61362.

[8] Lie, H., Mo, K., Vandiver, K., "VIV Model Test of Bare- and Staggered Buoyancy Riser in a Rotating Rig", OTC, Houston, 1998

[9] Li, L., Fu, S., Yang, J., Ren, T. and Wang, X., "Experimental Investigation on Vortex-induced Vibration of Risers with Staggered Buoyancy", OMAE, Rotterdam, 2011.

[10] Jhingran, V., Zhang, H.P., Lie, H., Braaten, H., and Vandiver, J.K., "Buoyancy Spacing Implications for Fatigue Damage due to Vortex-Induced Vibrations on a Steel Lazy Wave Riser (SLWR)". Offshore Technology Conference, OTC23672, May 2012, Houston, USA.

[11] Passano, E., Larsen, C.M., Lie, H., and Wu, J., (2014) VIVANA - Theory Manual Version 4.4.

[12] Rao, Z, Vandiver, K., and Jhingran, V., "VIV Excitation Competition Between Bare and Buoyant Segments of Flexible Cylinders", OMAE2013-11296, July 2013, Nates, France.

[13] Leijian Song, Shixiao Fu, Yadong Zeng, Yifan Chen. Hydrodynamic Forces and Coefficients on Flexible Risers Undergoing Vortex-Induced Vibrations in Uniform Flow. Journal of Waterway Port Coastal and Ocean Engineering, 2016, Vol.142, No. 4.

[14] Triantafyllou, M., Triantafyllou, G., David Tein, Y. S., & Ambrose, B. D. (1999). Pragmatic riser VIV analysis. Houston, USA: Offshore Technology Conference.

[15] Vandiver, J., & Li, L. (2007). Shear7 v4.5 Program Theoretical Manual. Cambridge: Massachusetts Institute of Technology.

[16] Venugopal, M. (1996). Damping and response prediction of a flexible cylinder in a current. Boston: Massachusetts Institute of Technology.

[17] Vikestad, K., Larsen, C., & Vandiver, J. (2000). Norwegian Deepwater Program Damping of Vortex-Induced Vibrations. Offshore Technology Conference, OTC11998. Houston, USA.

[18] Wu, J., 2011, Hydrodynamic Force Identification from Stochastic Vortex Induced Vibration Experiments with Slender Beams, PhD Dissertation, Norwegian University of Science and Technology, Trondheim.

[19] Wu, J., Lie, H., Constantinides, Y., & Baarholm, R. (2016a). NDP riser VIV model test with staggered buoyancy elements. Bushan, the South Korea: 35th International Conference on Ocean, Offshore and Arctic Engineering, OMAE2016-54503.

[20] Wu, J., & Fu, S. (2016b). NDP Staggered Buoyancy VIV Analysis - Advanced data analysis and prediction. Trondheim, Norway: SINTEF Ocean Report (Confidential).

[21] Wu J., Lie H., Larsen C. M., Liapis S. and Baarholm R., (2016c) Vortex-induced vibration of a flexible cylinder: Interaction of the in-line and cross-flow responses. Journal of Fluids and Structures 63:238-258, May 2016.

